Low-dose curcuminoid-loaded in dextran nanobubbles can prevent metastatic spreading in prostate cancer cells

(Article begins on next page)

20 March 2024

Low-dose curcuminoid-loaded in dextran nanobubbles can prevent metastatic spreading in prostate cancer cells

F Bessone [1,5], M Argenziano[1,5], G Grillo[1], B Ferrara[1], S Pizzimenti[2], G Barrera[2], G Cravotto[1], C Guiot[3], I Stura[4] , R Cavalli[1] and C Dianzani[1]

1 Department of Drug Science & Technology, University of Torino, Torino, Italy

2 Department of Clinical and Biological Sciences, University of Torino, Italy

3 Department of Neuroscience 'R. Levi Montalcini', University of Torino, Torino, Italy

4 Department of Public Health and Paediatric Sciences, University of Torino, Italy

5 These authors contributed equally to the work.

E-mail: ilaria.stura@unito.it

Abstract

Preventing recurrences and metastasis of prostate cancer after prostatectomy by administering adjuvant therapies is quite a controversial issue. In addition to effectiveness, absence of side effects and long term toxicity are mandatory. Curcuminoids (Curc) extracted with innovative techniques and effectively loaded by polymeric nanobubbles (Curc-NBs) satisfy such requirements. Curc-NBs showed stable over 30 d, were effectively internalized by tumor cells and were able to slowly release Curc in a sustained way. Significant biological effects were detected in PC-3 and DU-145 cell lines where Curc-NBs were able to inhibit adhesion and migration, to promote cell apoptosis and to affect cell viability and colony-forming capacity in a dose-dependent manner. Since the favourable effects are already detectable at very low doses, which can be reached at a clinical level, the actual drug concentration can be visualized and monitored by US or MRI, Curc-NBs can be proposed as an effective adjuvant theranostic tool.

Keywords: prostate cancer, nano*, curcumin, adjuvant therapy, theranostics

1.Introduction

Prostate cancer (PCa) is one of the most diffuse pathology in elderly men. Due to its very slow development and the chance of predicting it in advance, by monitoring the serum concentration of the prostate specific antigen (PSA), more than 3 over 4 patients recovers following surgical excision or radical radiotherapy [1]. However, in the cases of 'high risk PCa', that are often predictable as based on cancer histology, PSA values, etc, patients are at risk of developing local or metastatic (mainly in bones) recurrences, which can evolve in the almost noncurable castration resistant PCa [2]. To prevent or delay recurrences, such patients are normally treated with adjuvant therapies (i.e. concomitant or just following radical surgery or radiotherapy) mainly based on androgen deprivation therapies (ADT), although for adjuvant ADT in high risk patients neither conclusive support

for benefits [3] nor standard recommendations [4] exist. Since hormonal adjuvant therapies have many collateral toxic effects, especially for elderly or multi-diseased patients, there is a need for 'natural' and safe principles addressing new adjuvant therapies. A possible candidate, largely investigated and administered especially in the far East, is curcumin. Curcumin is a natural polyphenol molecule derived from the Curcuma longa L. plant. Research over the last two decades has shown curcumin to be a potent antioxidant, antiinflammatory, anti-angiogenic, anti-diabetic, hepatoprotective, anti-atherosclerotic, anti-thrombotic, and anti-arthritic agent in cell culture and animal studies [5]. Moreover, current preclinical and clinical studies revealed that curcumin also exerts antiproliferative and proapoptotic effects against various tumors in vitro and in vivo, and that it inhibits carcinogenesis of the breast and other organs [6]. Curcumin is able to interfere with the tumor cell cycle and inhibit tumor cell invasion through regulation of cytokines, growth factors and their receptors, enzymes, and adhesion molecules [6]. It induces apoptosis in cancer cells by inhibiting various intracellular transcription factors and secondary messengers such as NF-kB, AP-1, c-Jun, the Jak-STAT pathway and various others [7]. Moreover, several preclinical studies demonstrated that curcumin is also able to inhibit chemically induced carcinogenesis, both at initial and progression stages [8]. Furthermore, in the past decade, research about bioactivity of turmeric components has been broadened, opening new perspective about chemical entities different from curcuminoids (Curc). Curcumin-free extracts from turmeric, demonstrate different biological activities such as antidiabetic, anticancer, antimicrobial and anti-inflammatory effect [9]. Several investigations have been focused on the pharmacological properties of the lipophilic fraction (turmeric oil), mainly composed by aromatic (ar)-turmerone, alfa-turmerone, beta-turmerone, curlone, sesquiphellandrene, and zingiberene. This field of research was corroborated by the potent anticancer and anti-inflammatory activities discovered [10–12]. Although the biological effects of turmeric oil have been reported, its role as isolated fraction or as an extract component it is still not completely clarified. A synergistic effect of the whole phytocomplex with Curc seems to enhance the curcumin bioavailability [13]. Depending on the cultivar, on the origin and in general on the growing conditions, Curc content in Curcuma longa L. range from 2% to 9% [14, 15]. With such a low concentrated matrix, an efficient extraction procedure is mandatory, also considering the critical stability profile of Curc, given their proneness to photo- and oxidative degradation [16]. For these reasons microwave-assisted extraction (MAE) has been selected. Microwaves was introduced in the eighties for analytical samples preparation using domestic ovens [17]. MAE differs from conventional techniques, because the direct interaction of dielectric heating with the in situ water and other polar components within the cells of the plant material. The electromagnetic waves generate thermal energy by friction of oscillating dipoles and ions with consequent cell membranes and walls rupture and the release of target compounds [18]. The efficiency of microwaves to be converted into heat is expressed by the dielectric properties of the material, and for this reason particular importance is played by the solvent [19]. In conventional processes heat moves from the hot solvent to the inner part of the matrix, whilst in MAE the heat is transferred volumetrically within the irradiated medium, allowing fast treatments and avoiding degradation. The sum of these peculiarities allows a synergistic combination of heat and

mass transport phenomena, leading to extraction acceleration and increasing selectivity and yields.

In summary, Curc is a good candidate due to some very positive features:

• anticancer, chemo-preventive, chemo-and radio-sensitization properties;

• widespread availability and safety; and

• low cost.

There are, however, also some contra: curcumin possess poor water solubility and lack of stability. Curcumin presents a rapid degradation by hydrolysis and then it undergoes molecular fragmentation [20]; as consequence, it exhibits low bioavailability. Moreover, it displays rapid intestinal and hepatic metabolism, indeed approximately 60%–70% of an oral dose of curcumin gets eliminated in the feces [21]. Moreover, several clinical studies showed that only few patients responded to curcumin despite high doses used. Moreover, the solubility, stability and consequently the bioavailability of curcumin can be enhanced by encapsulation in nanoparticles. Proper delivery vehicles should therefore be designed, and being the dosage at which curcumin is effective very critical point it should be monitorable in real time, suggesting that a theranostic nanocarrier would be the best choice. Many nanocarriers have already been proposed to deliver either curcumin alone or curcumin associated with antitumoral drugs. Restricting our attention on the first case, a WoS investigation found about 20 relevant related original papers. Experiments were performed on PCa cell lines (mainly LNCaP, PC-3 and DU-145) at various curcumin doses from 5 up to 600 μM. Direct curcumin administration produced dosedependent inhibition of cellular proliferation [22, 23], induction of apoptosis [23, 24] and direct cell toxicity at doses larger than 50 μM [25–28]. Such effects were detected also when curcumin was delivered by nanocarriers [25] but also other important features were underlined, as effective internalization [28] and enhanced anticancer effect [29–31]. Different theranostic nanocarriers have also been proposed so far based on the correlated imaging techniques mainly MRI [26, 32–35] and optical [36–39]. Nanobubbles with dextran sulfate-shell and perfluoropentane core can be designed for the delivery of Curc and tuned to efficiently encapsulate Curc in a large amount. Curcuminoid-loaded nanobubbles (Cur-NBs) were therefore developed as innovative delivery systems, able to carry and to release Curc to the target site. Moreover, nanobubble nanosuspensions can protect Curc from degradation and chemical instability that occur under physiological conditions [40]. Indeed, nanobubbles are interesting nano-tools that can store and enhance the stability of the carried drug or compound [41]. Being Curc-NBs detectable using ultrasound (US) imaging [42] and MRI [43], they are effective theranostic tools. In the present work, the effect of highly concentrated Curc extracts has been investigated both free and carried in nanobubbles as Curc-NBs. Nanobubbles are innovative nanoplatform developed with the aim to enhance the effectiveness of therapeutic treatments, control drug release, modify pharmacokinetics and biodistribution, decrease the administered doses of encapsulated drugs, overcome biological barriers, target specific cells and decrease the occurrence of side effects. Nanobubbles are core–shell structure and present spherical shape. Their

shell mainly consists of lipids, proteins, polymers or biocompatible polysaccharide (i.e. chitosan, or dextran sulfate), instead the core can be filled up with various gases, such as perfluorocarbons, sulphur hexafluoride, air and carbon dioxide. Nanobubbles have been deeply investigated as drug and nucleic acid delivery systems [41] and displayed effective oxygen storing capacity [44]. In addition to their drug loading capability, nanobubbles are US responsive nanocarriers [43]. Being US sensitive, this nanotechnology has been used for the development of externally triggered nanocarriers that provide controlled payload release. Interestingly, nano-sized bubbles can extravasate from blood vessels into surrounding tissues, thus improving the delivery efficiency and localization. Furthermore, nanoscale dimensions offer some advantages, such as the ability to accumulate within tumour tissues via the enhanced permeability and retention effect. In addition to the accumulation via passing targeting, nanobubbles can be functionalized and provide an active targeting. Indeed, binding antibodies to the nanobubble surface can direct the nanosystems in the target tissue, improving the therapeutic therapy efficacy. For this purpose, in order to provide a proof-of-concept about the effectiveness of Curc as adjuvant therapy to prevent PCa recurrence after radical prostatectomy or radiotherapy, when a small number of viable cancer cells are expected (comparable with in vitro samples), we designed dextranshelled Curc-NBs. We investigated Curc effect both in solution and as Curc-NBs on cell viability, colony formation, apoptosis, adhesion and migration properties in two PCa cells lines.

2. Materials and methods

2.1. Material

The substances and laboratory reagents were from Sigma- Aldrich (St Louis, MO, USA), unless otherwise specified. Soybean lecithin (Epikuron 200®) was kindly gifted by Degussa (Hamburg, Germany). Perfluoro-n-pentane min. 98% and was sourced from Strem Chemical (Newburyport, MA, USA). Ultrapure water was obtained using a 1–800 Millipore system (Molsheim, France). Tubular semi-permeable cellulose membrane was from Carl Roth (Karlsruhe, Germany). Cell culture reagents were purchased from Gibco/ Invitrogen (Life Technologies, Paisley, UK) except where otherwise indicated. All reagents were of analytical grade.

2.2. Methods

2.2.1. Preparation and characterization of Curc.

Curcuma longa L. rhizome powder (2 mm average size) was transferred into a 40 ml glass vessel. Hydroalcoholic solution (70% ethanol) was added keeping a solid–liquid ratio of 1:10. Extraction was performed into a multimodal microwave autoclave reactor (Synthwave, Milestone). With a fixed maximum power of 1500 W, sample was irradiated for 5min at 80 °C under magnetic stirring (650 rpm). The system was pressurized with N2 (2 bar) to prevent solvent evaporation and Curc degradation. The crude extract was filtered on sintered glass and dried under vacuum. Total Curc concentration was measured by HPLC with external standard calibration curve. Analysis was performed with a Waters 1525 binary HPLC pump equipped with 2998 PDA, and a Phenomenex Kinetex® Column

(5 μm C18 100 Å, 250×4.6 mm). Data acquisition was accomplished using Empower PRO (Waters Associates, Milford, CT, USA). CH3CN: 5% acetic acid aqueous solution was used as mobile phase. The chromatographic separation was performed in isocratic (50:50, v/v) at 25 °C with a flow rate of 1 ml min−1. Injection volume was 10 μl, while sample detection was carried out at 425 nm; Curc standard solutions (from 0.02 to 2 mgml−1) were analysed by HPLC (10 μl injection) to give linear regressions with R^2>0.999. Before the injection, all samples were dissolved in MeOH, giving concentrations of between 10 and 20 mg ml−1. All samples were filtered through 0.2 μm membrane filters before injection into the HPLC apparatus.

2.2.2. Preparation of curcuminoids solution. Solubility issue of Curc is a limitation for the preparation of a solution. Since Curc are poorly water soluble, an organic solvent is required. Moreover, the choice of the solvent should be taken considering its application in biological studies. For this purpose, N-methyl-2-pyrrolidone was selected. Curc solution was obtained by firstly solving a weighted amount of Curc at a concentration of 0.5M in N-methyl-2-pyrrolidone. Then, the solution was diluted in a mixture of N-methyl-2-pyrrolidone/0.9% NaCl in a ratio 1:1, to obtain a final concentration of 3 mM. The Curc concentration of the solution was determined by a RF-551 Spectrofluorometer (Shimadzu, Kyoto, Japan) using the method described below. Once obtained, the Curc solution was stored at 4 °C.

2.2.3. Preparation of unloaded nanobubbles. NBs were obtained by tuning a previously described method [44–46]. NBs were prepared using perfluoropentane as inner core component and dextran sulfate salt (MW of 100 kDa) for the shell. At the beginning, 350 μl of an ethanol solution containing Epikuron® 200 (1.5% w/v) was added to 450 μl of perfluoropentane forming a pre-emulsion. Then, ultrapure water was added the mixture was homogenized using an Ultra-Turrax® homogenizer (IKA, Konigswinter, Germany) for 2 min and heat at 37 °C for 15 min. After that, an aqueous solution of the dextran sulfate salt (2% w/v) was added dropwise under mild magnetic stirring. Blank NBs were used as control in the following experiments.

2.2.4. Preparation of curcuminoid-loaded nanobubbles. Curc-NBs were prepared adding to an ethanol solution containing Epikuron® 200 (1.5% w/v) Curc (8.5% w/v). After the addition of perfluoropentane and ultrapure water, the mixture was homogenized using an Ultra-Turrax® homogenizer for 2 min and heat at 37 °C for 15 min. Then, an aqueous solution of the dextran sulfate salt (2% w/v) was added dropwise under mild magnetic stirring. The final concentration of loaded Curc in the formulation was 3 mM, determined by Spectrofluorometer analysis using the method described below.

2.2.5. Characterization of nanobubble formulations. The different NB formulations were physico-chemically characterized. The nano-suspensions were previously diluted in deionized filtered water. Then, the average diameters and polydispersity indices of the various diluted nanobubble formulations were measured by photocorrelation spectroscopy using a 90 Plus instrument (Brookhaven, New York City, NY, USA) with a scattering angle of 90° at 25 °C. The zeta potential was determined by the same instrument. The diluted

samples, placed in an electrophoretic cell, were subjected to an electric field of around 15V cm−1. The analyses were conducted in triplicate of three different batches.

2.2.6. Spectrofluorometer quantitative curcuminoid determination method. Curc concentration was determined using a RF-551 Spectrofluorometer (Shimadzu, Kyoto, Japan). The excitation wavelength was set 422 nm and the emission spectrum was recorded in a wavelength range between 350 and 650 nm. The peak area correlated linearly with Curc concentration in the range of 5–30 ng ml−1 (R^2=0.9994). To calculate Curc concentration, a linear calibration curve was set up with a concentration range of 2.5–30 ng ml−1 (R2=0.9994).

2.2.7. Echogenic properties of nanobubble formulations. Echogenic images were visualized using MyLab 25Gold (Esaote, Genova, Italy) instrument. The frequency was 7.5 MHz; contrast Res modality.

2.2.8. Encapsulation efficiency and loading capacity of curcuminoids in nanobubbles. Curc-NB encapsulation efficiency was determined with a centrifugal filter system. For this purpose, 100 µl of Curc-NB formulation were put in an centrifugal filter device (Amicon® Ultra-0.5) and then centrifuged at 20 000 rpm for 15 min with a Beckman Coulter Allegra 64R Centrifuge. The filtered solution was collected and the amount of free Curc in the nanosuspension was quantified by a spectrofluorometer. The encapsulation efficiency was calculated as follows:

$$\text{Encapsulation Efficiency} = \left(\frac{Total\ Curc - Free\ Curc}{Total\ Curc}\right) * 100$$

Freeze-dried NB samples were used for the determination of the loading capacity. A weighted amount of freeze-dried Curc-NBs was suspended in water. The sample was firstly sonicated and centrifuged, and then the supernatant was analyzed. The loading capacity of Curc in Curc-NBs was calculated as follows:

$$\text{Loading Capacity} = \left(\frac{Total\ Curc - Free\ Curc}{NB\ weight}\right) * 100$$

2 2.2.9. In vitro curcuminoid release from curcuminoids-nanobubbles. The in vitro release of Curc from nanobubble formulation was carried out by the use a multi-compartment rotating cell. Curc-NBs and Curc solution as control were respectively placed in the donor chambers, separated from the receiving chamber by a semipermeable cellulose membrane (cut-off 14 kDa). The receiving phase consisted of a H2O/EtOH 1:1 mixture. At fixed time intervals, the samples were collected and the same volume was replaced with fresh receiving phase. Then, the samples were analyzed and Curc concentration was determined by Spectrofluorometer, following the method described above.

2.2.10. In vitro evaluation of chemical stability of curcuminoid solution and curcuminoid-nanobubbles over time. The chemical stability of Curc was evaluated in N-methyl-2-

pyrrolidone/0.9% NaCl solution and carried in nanobubbles. The concentration over time was then evaluated by spectrofluorometry, following the method described above. The samples were stored at 4 °C and analysed up to 30 d.

2.2.11. Cells. Human umbilical vein endothelial cells (HUVEC) were isolated from human umbilical veins by collagenase treatment (1%) and cultured in M199 medium with the addition of 20% fetal calf serum (FCS) 100 UI ml−1 penicillin, 100 µgml−1 streptomycin, 5 UI ml−1 heparin, 12 µgml−1 bovine brain extract and 200mM glutamine. HUVEC were grown to confluence in flasks and used from the second to the fifth passage [47]. Use of HUVEC was approved by the Ethics Committee of the 'Presidio Ospedaliero Martini' of Turin and conducted in accordance to the Declaration of Helsinki. Written informed consent was obtained from all donors. The study was performed on two prostate cell line, PC-3 and DU-145. The cell lines were grown in culture dishes as a monolayer in RPMI 1640 medium plus 10% FCS, 100 U ml−1 penicillin, and 100 µgml−1 streptomycin at 37 °C in a 5% CO2 humidified atmosphere.

2.2.12. Curcuminoids-nanobubble cell uptake. PC-3 cells were seeded onto Corning® cover glasses (Sigma) in a 24-well plate (4×10^4 cells per well) and incubated overnight at 37 °C in a 5% CO2 atmosphere. Then, the media was replaced with a fresh media mixture containing Curc-NBs and free Curc in solution, both at a final concentration of 5 µM. After 1 h of incubation, the cells were washed with PBS, and fixed in 4% paraformaldehyde at room temperature for 15 min. Fixed cells were washed with PBS and stained with 4′,6-diamidine-2-phenylindole. Finally coverslips were mounted. Image acquisition was performed with a TCS SP2 AOBS confocal microscope (Leica, Wetzlar, Germany), equipped with 63X/1.40 HCX Plan-Apochromat oil-immersion objective.

2.2.13. In vitro cytotoxicity studies. The human tumor cells, PC-3 and DU-145, were obtained from ATCC (Milan, Italy) and used to perform in vitro cytotoxicity test. Cells (800/well) were seeded in 96-well plates and incubated at 37 °C, 5% CO2 for 24 h in RPMI 1640 media. Then, the cells were treated with blank NBs, Curc solution and Curc-NBs at a concentration in the range 1–15 µM. After 24–72 h incubation, viable cells were evaluated by 2,3-bis[2-methoxy-4-nitro-5sulphophenyl]-2Htetrazolium- 5carboxanilide (MTT) inner salt reagent at 570 nm, as described by the manufacturer's protocol. The controls cells were normalized to 100%, and the readings from treated cells were expressed as % of viability inhibition. Eight replicates were used to determine each data point and five different experiments were performed.

2.2.14. Colony-forming assay. PC-3 and DU-145 cells (800/ well) were seeded into six-well plates and treated with blank NBs, Curc solution and Curc-NBs (1–15 µM). The medium was changed after 3–24 h and cells were cultured for additional 10 d. Subsequently, cells were fixed and stained with a solution of 80% crystal violet and 20% methanol. Colonies were washed and 30% acetic acid were added to induce a complete dissolution of the crystal violet. Absorbance was recorded at 595 nm by a 96-well-plate ELISA reader. Five different experiments were performed. The controls (untreated cells) were normalized to 100%, and the readings from treated cells were expressed as % of viability inhibition.

2.2.15. Cell apoptosis assay. The cell apoptosis was detected by using the FITC Annexin V Apoptosis Detection Kit (BD Biosciences Cat N° 556 547). Briefly, PC-3 cells (120.000/well) were seeded into six-well plates and treated with blank NBs, Curc solution, or Curc-NBs (10 and 15 µM). After 24 h, adherent and non-adherent treated and control cells were harvested and stained with FITC-Annexin V and PI, according to the manufacturer protocol. The samples were analyzed with a FACScan cytometer (Becton Dickinson, Accuri).

2.2.16. Cell adhesion assay. HUVEC were grown to confluence in 24-well plates. Then, cells were pre-treated for 30 min with blank NBs, Curc solution and Curc-NBs at a concentration of 5 µM and then were stimulated with TNF-α 10 ng ml−1. After 18 h HUVEC were washed twice with fresh medium and tumor cells (1×10^5 cells/well) were seeded and left to adhere with HUVEC for 1 h, as previously reported [48]. Unattached tumor cells were washed away and the number of adherent cells was evaluated by the Image Pro Plus Software for micro-imaging (Media Cybernetics, version 5.0, Bethesda, MD, USA). Viability of the unattached cells was evaluated by the Trypan Blu test. Five different experiments were performed. Data are shown as percentages of the adhesion of treated cells. Control adhesion was 49±4 cells per microscope field for PC-3 cells and in a similar range (54 ± 5 cells) for DU-145 (mean ± standard error of the mean (SEM)).

2.2.17. Cell motility assay. In the Boyden chamber invasion assay, cells (5 × 103) were plated onto the apical side as previously reported [49] in serum-free medium with blank NBs, Curc solution and Curc-NB (5 µM). Medium containing PMA 100 ng ml−1 or FCS 20% were placed in the basolateral chamber as chemoattractants. After 18 h, cells on the apical side were wiped off with Q-tips. Cells on the bottom of the filter were stained with crystal-violet and counted (all fields of each triplicate filter) with an inverted microscope. Five different experiments were performed. Data are shown as percentages of the migration of treated cells. Control migration was 52±4 cells per microscope field for PC-3 cells and 66±5 for DU-145 cells. 2.2.18. Data analysis. Data are shown as mean±SEM. Statistical analyses were performed with GraphPad Prism 5.0 software (San Diego, CA, USA). One way ANOVA was performed, followed by Tukey's multiple comparison posttest when needed. Only P values<0.05 were considered to be significant.

3. Results

3.1. Preparation and characterization of the curcuminoids The highly efficient MW-assisted extraction procedure afforded 20.76% of Curc (12.49% Curc, 4.77% demethoxycurc, 3.50% bisdemethoxycurc) in the dry extract, besides other bioactive lipophilic compounds (terpenes and terpenoids fully characterized by GC-MS—data not reported here). The reported yield represent nearly the 90% of the total content in rhizomes. The fast process (5 min) and the controlled atmosphere helped to preserve the activity of the final extract, which has been used without any further purification. 3.2. Characterization of nanobubble formulations NB with dextran sulfate-shell and perfluoropentane core were designed for the delivery of Curc. Novel NB formulations were tuned to efficiently encapsulate Curc in a

large amount. Cur-NBs were developed as innovative delivery systems, able to carry and to release Curc to the target site. Moreover, NB nano-suspensions can protect Curc from degradation and chemical instability that occur under physiological conditions [40]. Indeed, NB are interesting nanotools that can store and enhance the stability of the carried drug or compound [41, 46]. Curc-NBs were formulated and blank NBs were used as control. The average diameters, polydispersity indices, zeta potentials, and pH of Curc-loaded and unloaded NB formulations are reported in table 1. Curc-NB and blank NB both presented a mean diameter of less than 350 nm and negative Z-potential, due to the negative charges of destran sulfate. The pH of the nano-suspensions is accepted and applied in biological systems.

3.3. Encapsulation efficiency and loading capacity of curcuminoids in nanobubbles NBs were able to efficiently encapsulate Curc, with an encapsulation efficiency of 97% (see equation (1)) On the other hand, the loading capacity of Curc-NBs was of 14.20% (see equation (2)).

3.4. In vitro curcuminoids release from curcuminoidsnanobubbles The in vitro Curc release from Curc-NBs and Curc solution was comparatively evaluated over time up to 28 h. Curc-NBs displayed a slower and prolonged Curc release over time, in respect to Curc solution (see figure 1). After 24 h, only 25% of the Curc was released from Curc-NBs. Thus, it might be hypnotized that Curc-NBs act as a reservoir of the compound until they reach the target site.

3.5. In vitro evaluation of chemical stability of curcuminoids Curc stability was evaluated in N-methyl-2-pyrrolidone solution and when loaded in NBs. The Curc concentration in the NBs was stable up to 1 month. It means that the encapsulation of Curc in the nano-formulation increased the chemical stability of the compounds compared to free Curc (see figure 2). Indeed, the decrease in absorbance over time occurred much faster for the Curc solution, reaching a 60% decrease of the concentration after 30 d.

3.6. Curcuminoids-nanobubbles display echogenic properties Curc-loaded NB echogenic properties were visualized by US imaging (see figure 3).

3.7. Curcuminoids-nanobubbles cell internalization In order to evaluate the biological uptake, Curc-NBs and Curc solution were incubated at a concentration of 5 μM with PC-3 cell line for 1 h. Exploiting Curc fluorescence per se, the internalization was evaluated by confocal microscopy. As reported in figure 4, Curc-NBs were avidly internalized by the cells compared to free Curc.

3.8. Viability test We compared the ability of Curc solution and Curc-NBs to inhibit the growth of PC-3 and DU-145 cells in vitro, as explained in the section 2. Table 2 shows that in both cell lines Curc-NBs inhibited cell viability to a higher extent than Curc. The effect was concentration- and time-dependent with small difference between the two cell lines. Curc-NBs were more efficient than Curc solution in terms of timing, maximal inhibition and effective doses. At small doses, on the contrary, Curc are almost non-toxic either in free form or encapsulated. Blank NBs had no effect on tumor cell viability at all the concentrations and the times tested.

3.9. Colony-forming assay To validate MTT results, we performed colony-forming assay. MTT test only reveals the metabolic activity of the cells, indeed, to demonstrate the real ability of the cells to proliferate after the exposition to the tested compounds, we used the colony-forming assay. It is an in vitro cell survival assay based on the ability of a single cell to growth into a colony as described in the section 2. After plating the cells at very low density (800 cells for wells, using 6-well-plates), cells are treated for 3 or 24 h with the compounds, then they were removed by washing the cells with the cell medium, allowing the cells to growth for 7 d in a free medium. Therefore, only cells with a still functioning reproductive system will be able to proliferate. Results demonstrated that there are significant difference between PC-3 cells treated with Curc solution and Curc-NBs already after 3 h at the higher doses, while the higher efficacy of Curc-NBs become constant at all the concentration tested after 24 h (figure 5(a)). Similar results were obtained with DU-145 cell line (data not shown), demonstrating the higher and faster internalization of the Curc loaded in NB. Figure 5(b) shows assay photos from a representative experiments.

3.10. Cell apoptosis The Annexin V-FITC/IP Apoptosis assay results are presented in figure 6. The flow cytometry profiles of a representative experiment is shown in panel (A). The PC-3 untreated cells and the cells exposed to blank NBs, at the dilution corresponding to that of Curc-NBs 15 µM, showed a cell viability of 95.5% and 90%, respectively. Treatment with 10 and 15 µM Curc solution induced a significant increase of annexin V-positive cells (19.6% and 35.6%, respectively). The percentage of apoptotic cells was further increased when the cells were treated with Curc-NBs at the same concentrations (41% and 54.2% in Curc- NBs 10 µM and Curc-NBs 15 µM, respectively). In figure 6(b) the summary of the Annexin V-FITC Apoptosis assay results of three independent experiments are shown.

3.11. Adhesion test Adhesion of tumor cells to vascular endothelium and their migration to the target organs are key steps for metastasis formation. In vitro experiments were performed on adhesion to HUVEC and motility of tumor cell to compare the antimetastatic potential of free Curc and Curc-NBs (see details in section 2). In the adhesion experiments, HUVEC were pretreated for 30 min with blank NBs, Curc solution, and Curc-NB (5 µM) and then were stimulated with TNF-α 10 ng ml−1. After 18 h tumor cells were seeded and left to adhere with HUVEC for 1 h. 5 µM of Curc solution or Curc- NBs were chosen in these experiments of adhesion and migration, because this concentration resulted to be non-toxic for tumor cells. Results shown in figure 7 showed that low dose Curc can completely reverse the pro-adhesional effect of TNF-α in DU-145 cells and PC-3 cells, respectively, being Curc-NBs significantly more effective than free Curc. 3.12. Migration test Cell motility was assessed using a Boyden chamber assay assessing directional migration and invasion of cells. DU-145 and PC-3 cells were seeded in the upper chamber of a Boyden chamber in a serum-free medium, to avoid cell proliferation, in the presence of blank NBs or 5 µM of Curc solution or Curc-NBs. Then, cells were allowed to migrate for 18 h to the lower chamber containing PMA or 10% FCS, used as chemoattractants. Figure 8 shows that cell migration is dramatically reduced per-se and in presence of pro-migration substance at low Curc concentrations. Moreover, the effect was

larger when Curc are loaded in nanobubbles, in both DU-145 and PC-3 cell lines, respectively.

4. Discussion

Curcumin is currently administered orally but its low bioavailability needs high doses. In this work, we would like to overcome this drawbacks with a two-fold approach: the use of a Curc extract and its incorporation in a nanocarrier. The first problem is a non-trivial one. Indeed, in food and pharmaceutical applications a restricted number of solvents are allowed for the extraction process (FAO/WHO and European Commission sources), comprising, according to different polarity, ethanol, methanol, acetone, hexane and ethyl acetate [50]. Ethanol is commonly the most preferred solvent in turmeric extraction, ensuring good yields and purity in curcumin [14]. Among the enabling technologies that can ensure a rapid and cost-effective recovery of bioactives from vegetal matrices [51], microwave irradiation represents a promising method to enhance extraction efficiency and selectivity [52] compared to conventional thermal heating, boosting extraction and reducing time and solvents. Fast protocols are critical in handling labile metabolites and avoiding losses or degradations. Here, we tuned a new extraction method to obtain Curc extract with high purity and safety. The second point was focused by selecting dextran-based NBs, a versatile nanotool suitable for different administration routes and with echogenic properties. NBs are spherical nanoparticles with a core–shell structure filled up with a gas, which gives them acoustically active properties. With this aim, NBs were largely proposed as theranostic agents, combining the modality of therapy and diagnostic imaging [43, 53, 54]. In particular, polymer-shelled NBs were designed as multifunctional agents with the aim to provide tumor cell targeting, US imaging and US-triggered cancer therapy [55–57]. The theranostic approach offers the potential to image the pathological tissues and simultaneously to monitor the delivery kinetics and biodistribution of an active compound. Previously, curcumin was delivered in PEG-PCL nanodroplets showing an enhanced anticancer effect in mice [58]. Once injected, these nanodroplets based on perfluoropentane accumulated in sarcoma tumor tissue and were disrupted by US, releasing curcumin. Curcumin-loaded nanodroplets significantly reduced the primary tumor volume compared to the control, in a greater extent when activated by US. Nevertheless, no in vitro studies were carried out and the possible rule of the nanodroplets on the occurrence of metastasis was not investigated. More recently, microbubbles loading curcumin were synthesized using bovine serum albumin as shell component and perfluorobutane as gas core [59]. Curcumin uptake by HeLa cells increased when the active compound was carried on the microbubbles. Moreover, the cell viability reduced significantly when the microbubbles were used with US supply. Besides, microbubbles cannot passively extravasate from blood vessels into surrounding tissues due to their size. In this work, we focused the attention on prostatic cell lines, PC-3 and DU-145, designing nanoscale systems for potentially impairing metastatic spread. It is worth noting that, in order to prevent or delay recurrences, the patients are normally treated with adjuvant therapies (radical surgery or radiotherapy), although frequently they are not conclusive. In vitro results showed that Curc alone was effective in inhibiting PCa cell growth, colony-

forming ability, endothelial adhesion and migration. We speculated that the concomitant presence of demethoxycurcumin, bisdemethoxycurcumin and other bioactive lipophilic compounds presented in Curcuma longa L. extract can play a role in the enhanced effectiveness of Curc with respect to curcumin. In particular, Curc effect at highest concentration (15 µM) is detectable after 24 h of incubation, while after 48–72 h also 10 µM concentration become effective. In addition, Curc were able to reduce cell colony forming at all dosages, but only after 24 h of incubation. Moreover, Curc extract prevented adhesion to HUVEC and migration in the presence of promoting agents (TNF-alpha and PMA respectively) already at low concentration. Differences in concentration/effect is important since a therapeutic effect (i.e. preventing metastases formation) can be obtained avoiding toxicity (limited cell viability) to the nearby tissues. Such promising features were somehow enhanced whether Curc were delivered via nanobubbles forming the Curc- NBs systems, which were avidly internalized by cells (see figure 4). As a matter of fact, Curc-NBs inhibited cell viability and colony formation even at low doses and their effect, begun after 3 h and last for 24–48 h, suggests that Curc efficiency was preserved and 'protected' by the shell and that the active principle was fast internalized and slowly and gradually released. Interestingly, at low dose (5 µM) Curc-NBs showed a higher effect than Curc on cell motility, showing that Curc- Nbs may play a role against metastatic spread. As far as the adhesion properties are concerned, superficial differences between Curc in solution and carried in NBs may explain the different effectiveness, but in both cases adhesion was inhibited with respect to control. Our results are complementary with those reported by Dorai et al [24], that showed that curcumin was able to interfere with the osteoblastic as well as the osteoclastic component of the highly metastatic C4–2B PCa cell line, by interfering with the growth factor receptor pathways and by inhibiting the NF-kappaB activation process. Such result was confirmed by further investigations on PC-3 PCa cells, where the chemotactic activity of the CC motif ligand 2 was severely reduced by curcumin, inhibiting their pro-metastatic effectiveness [60]. More recently, it was observed that [61] curcumin abrogated HGF-induced cell scattering and invasion in DU-145 PCa cells by downregulating the expression of phosphorylated c-Met, extracellular signal-regulated kinase and Snail.

5. Conclusions

Based on the results of this study, Curc-NBs might be proposed as a safe and potential effective adjuvant therapy for preventing metastatic spread as an alternative to ADT. Since it has been reported that Cur-NBs have theranostic properties, their administration can be monitored and properly tailored in order to reach an effective release of Curc when residual cancer cells are suspected. Future in vivo studies are required to assess whether an effective dose (5 µM) can be reached in PCa cells following systemic and/or local administration.

Acknowledgments

ORCID iDs

I Stura https://orcid.org/0000-0001-9815-5446

References

[1] Stura I, Ditaranto S, Gabriele D, Migliaretti G and Guiot C 2017 A new predictive tool for the post-surgical risk of recurrence of prostate cancer potentially unveiling hidden residual disease J. Pros. Cancer 2 2

[2] Attard G, Parker C, Eeles R A, Schröder F, Tomlins S A, Tannock I, Drake C G and de Bono J S 2016 Prostate cancer Lancet 387 70–82

[3] Kumar S, Shelley M, Harrison C, Coles B, Wilt T J and Mason M D 2006 Neo-adjuvant and adjuvant hormone therapy for localised and locally advanced prostate cancer Cochrane Database Syst. Rev. 4 CD006019

[4] NCCN-Evidence-Based Cancer Guidelines, Oncology Drug Compendium, Oncology Continuing Medical Education www.nccn.org (accessed: 13 February 2019)

[5] Bansal S S, Goel M, Aqil F, Vadhanam M V and Gupta R C 2011 Advanced drug delivery systems of curcumin for cancer chemoprevention Cancer Prevention Res. 4 1158–71

[6] Bachmeier B E, Killian P H and Melchart D 2018 The role of curcumin in prevention and management of metastatic disease Int. J. Mol. Sci. 19 1716–34

[7] Anand P et al 2008 Biological activities of curcumin and its analogues (congeners) made by man and mother nature Biochem. Pharmacol. 76 1590–611

[8] Thangapazham R L, Sharma A and Maheshwari R K 2006 Multiple molecular targets in cancer chemoprevention by curcumin AAPS J. 8 E443–9

[9] Gupta S C, Sung B, Kim J H, Prasad S, Li S and Aggarwal B B 2013 Multitargeting by turmeric, the golden spice: from kitchen to clinic Mol. Nutrition Food Res. 57 1510–28

[10] Aratanechemuge Y, Komiya T, Moteki H, Katsuzaki H, Imai K and Hibasami H 2002 Selective induction of apoptosis by ar-turmerone isolated from turmeric (curcuma longa L) in two human leukemia cell lines, but not in human stomach cancer cell line Int. J. Mol. Med. 9 481–4

[11] Yue G G L, Chan B C L, Hon P-M, Lee M Y H, Fung K-P, Leung P-C and Lau C B S 2010 Evaluation of in vitro antiproliferative and immunomodulatory activities of compounds

isolated from curcuma longa Food Chem. Toxicol. Int. J. Publ. Br. Ind. Biol. Res. Assoc. 48 2011–20

[12] Sandur S K, Pandey M K, Sung B, Ahn K S, Murakami A, Sethi G, Limtrakul P, Badmaev V and Aggarwal B B 2007 Curcumin, demethoxycurcumin, bisdemethoxycurcumin, tetrahydrocurcumin and turmerones differentially regulate anti-inflammatory and anti-proliferative responses through a ROS-independent mechanism Carcinogenesis 28 1765–73

[13] Aggarwal B B, Yuan W, Li S and Gupta S C 2013 Curcuminfree turmeric exhibits anti-inflammatory and anticancer activities: identification of novel components of turmeric Mol. Nutrition Food Res. 57 1529–42

[14] Esatbeyoglu T, Huebbe P, Ernst I M A, Chin D, Wagner A E and Rimbach G 2012 Curcumin–from molecule to biological function Angew. Chem., Int. Ed. Engl. 51 5308–32

[15] Priyadarsini K I 2014 The chemistry of curcumin: from extraction to therapeutic agent Molecules 19 20091–112

[16] Peram M R, Jalalpure S S, Palkar M B and Diwan P V 2017 Stability studies of pure and mixture form of curcuminoids by reverse phase-HPLC method under various experimental stress conditions Food Sci. Biotechnol. 26 591–602

[17] Ganzler K, Salgó A and Valkó K 1986 Microwave extraction. A novel sample preparation method for chromatography J. Chromatogr. 371 299–306

[18] Chemat F and Cravotto G 2013 Microwave-assisted Extraction for Bioactive Compounds: Theory and Practice (New York, Heidelberg, Dordrecht, London: Springer)

[19] Cravotto G and Carnaroglio D 2017 Microwave Chemistry (Berlin, Boston: De Gruyter)

[20] Mondal S 2016 Stability of curcumin in different solvent and solution media: UV-visible and steady-state fluorescence spectral study J. Photochem. Photobiol. B 158 212–8

[21] Pan M H, Huang T M and Lin J K 1999 Biotransformation of curcumin through reduction and glucuronidation in mice Drug Metab. Dispos. Biol. Fate Chem. 27 486–94

[22] Dorai T, Dutcher J P, Dempster D W and Wiernik P H 2004 Therapeutic potential of curcumin in prostate cancer: IV. Interference with the osteomimetic properties of hormone refractory C4-2B prostate cancer cells Prostate 60 1–17

[23] Hong J H, Ahn K S, Bae E, Jeon S S and Choi H Y 2006 The effects of curcumin on the invasiveness of prostate cancer in vitro and in vivo Prostate Cancer Prostatic Dis. 9 147–52

[24] Mukerjee A and Vishwanatha J K 2009 Formulation, characterization and evaluation of curcumin-loaded PLGA nanospheres for cancer therapy Anticancer Res. 29 3867–75

[25] Adahoun M A, Al-Akhras M-A H, Jaafar M S and Bououdina M 2017 Enhanced anti-cancer and antimicrobial activities of curcumin nanoparticles Artif. Cells Nanomed. Biotechnol. 45 98–107

[26] Barick K C, Ekta, Gawali S L, Sarkar A, Kunwar A, Priyadarsini K I and Hassan P A 2016 Pluronic stabilized Fe3O4 magnetic nanoparticles for intracellular delivery of curcumin RSC Adv. 6 98674–81

[27] Salehi P, Makhoul G, Roy R, Malhotra M, Mood Z A and Daniel S J 2013 Curcumin loaded NIPAAM/VP/PEG-A nanoparticles: physicochemical and chemopreventive properties J. Biomater. Sci. Polym. Ed. 24 574–88

[28] Serri C et al 2017 Nano-precipitated curcumin loaded particles: effect of carrier size and drug complexation with (2-hydroxypropyl)-β-cyclodextrin on their biological performances Int. J. Pharm. 520 21–8

[29] Rao W et al 2014 Thermally responsive nanoparticleencapsulated curcumin and its combination with mild hyperthermia for enhanced cancer cell destruction Acta Biomater. 10 831–42

[30] Thangavel S, Yoshitomi T, Sakharkar M K and Nagasaki Y 2015 Redox nanoparticles inhibit curcumin oxidative degradation and enhance its therapeutic effect on prostate cancer J. Control. Release Off. J. Control. Release Soc. 209 110–9

[31] Yallapu M M, Dobberpuhl M R, Maher D M, Jaggi M and Chauhan S C 2012 Design of curcumin loaded cellulose nanoparticles for prostate cancer Curr. Drug Metab. 13 120–8

[32] Sivakumar B, Aswathy R G, Romero-Aburto R, Mitcham T, Mitchel K A, Nagaoka Y, Bouchard R R, Ajayan P M, Maekawa T and Sakthikumar D N 2017 Highly versatile SPION encapsulated PLGA nanoparticles as photothermal ablators of cancer cells and as multimodal imaging agents Biomater. Sci. 5 432–43

[33] Khalkhali M, Sadighian S, Rostamizadeh K, Khoeini F, Naghibi M, Bayat N, Habibizadeh M and Hamidi M 2015 Synthesis and characterization of dextran coated magnetite nanoparticles for diagnostics and therapy BioImpacts 5 141–50

[34] Yallapu M M, Othman S F, Curtis E T, Bauer N A, Chauhan N, Kumar D, Jaggi M and Chauhan S C 2012 Curcumin-loaded magnetic nanoparticles for breast cancer therapeutics and imaging applications Int. J. Nanomed. 7 1761–79

[35] Yallapu M M, Othman S F, Curtis E T, Gupta B K, Jaggi M and Chauhan S C 2011 Multi-functional magnetic nanoparticles for magnetic resonance imaging and cancer therapy Biomaterials 32 1890–905

[36] Mukerjee A, Ranjan A P and Vishwanatha J K 2016 Targeted nanocurcumin therapy using annexin A2 anitbody improves tumor accumulation and therapeutic efficacy against highly metastatic breast cancer J. Biomed. Nanotechnol. 12 1374–92

[37] Xue P, Liu D, Wang J, Zhang N, Zhou J, Li L, Guo W, Sun M, Han X and Wang Y 2016 Redox-sensitive citronellolcabazitaxel conjugate: maintained in vitro cytotoxicity and self-assembled as multifunctional nanomedicine Bioconjug. Chem. 27 1360–72

[38] Gong G, Pan Q, Wang K, Wu R, Sun Y and Lu Y 2015 Curcumin-incorporated albumin nanoparticles and its tumor image Nanotechnology 26 045603

[39] Verderio P, Pandolfi L, Mazzucchelli S, Marinozzi M R, Vanna R, Gramatica F, Corsi F, Colombo M, Morasso C and Prosperi D 2014 Antiproliferative effect of ASC-J9 delivered by PLGA nanoparticles against estrogendependent breast cancer cells Mol. Pharm. 11 2864–75

[40] Kharat M, Du Z, Zhang G and McClements D J 2017 Physical and chemical stability of curcumin in aqueous solutions and emulsions: impact of pH, temperature, and molecular environment J. Agric. Food Chem. 65 1525–32

[41] Cavalli R, Bisazza A, Trotta M, Argenziano M, Civra A, Donalisio M and Lembo D 2012 New chitosan nanobubbles for ultrasound-mediated gene delivery: preparation and in vitro characterization Int. J. Nanomed. 7 3309–18

[42] Capece S, Chiessi E, Cavalli R, Giustetto P, Grishenkov D and Paradossi G 2013 A general strategy for obtaining biodegradable polymer shelled microbubbles as theranostic devices Chem. Commun. 49 5763–5

[43] Cavalli R, Argenziano M, Vigna E, Giustetto P, Torres E, Aime S and Terreno E 2015 Preparation and in vitro characterization of chitosan nanobubbles as theranostic agents Colloids Surf. B 129 39–46

[44] Cavalli R, Bisazza A, Giustetto P, Civra A, Lembo D, Trotta G, Guiot C and Trotta M 2009 Preparation and characterization of dextran nanobubbles for oxygen delivery Int. J. Pharm. 381 160–5

[45] Marano F, Argenziano M, Frairia R, Adamini A, Bosco O, Rinella L, Fortunati N, Cavalli R and Catalano M G 2016 Doxorubicin-loaded nanobubbles combined with extracorporeal shock waves: basis for a new drug delivery tool in anaplastic thyroid cancer Thyroid Off. J. Am. Thyroid Assoc. 26 705–16

[46] Argenziano M et al 2017 Vancomycin-loaded nanobubbles: a new platform for controlled antibiotic delivery against methicillin-resistant staphylococcus aureus infections Int. J. Pharm. 523 176–88

[47] Gigliotti C L et al 2016 In vitro and in vivo therapeutic evaluation of camptothecin-encapsulated β-cyclodextrin nanosponges in prostate cancer J. Biomed. Nanotechnol. 12 114–27

[48] Gigliotti C L et al 2017 Enhanced cytotoxic effect of camptothecin nanosponges in anaplastic thyroid cancer cells in vitro and in vivo on orthotopic xenograft tumors Drug Deliv. 24 670–80

[49] Dianzani C et al 2014 B7h triggering inhibits the migration of tumor cell lines J. Immunol. 192 4921–31

[50] Anon 2010 Scientific Opinion on the re-evaluation of curcumin (E 100) as a food additive EFSA J. 8 1679

[51] Chemat F, Vian M A and Cravotto G 2012 Green extraction of natural products: concept and principles Int. J. Mol. Sci. 13 8615–27

[52] Cravotto G, Boffa L, Mantegna S, Perego P, Avogadro M and Cintas P 2008 Improved extraction of vegetable oils under high-intensity ultrasound and/or microwaves Ultrason. Sonochem. 15 898–902

[53] Zullino S, Argenziano M, Stura I, Guiot C and Cavalli R 2018 From micro- to nano-multifunctional theranostic platform: effective ultrasound imaging is not just a matter of scale Mol. Imaging 17 1–16

[54] Ayodele A T, Valizadeh A, Adabi M, Esnaashari S S, Madani F, Khosravani M and Adabi M 2017 Ultrasound nanobubbles and their applications as theranostic agents in cancer therapy: a review Biointerface Res. Appl. Chem. 7 2253–62

[55] Li Y, Wan J, Zhang Z, Guo J and Wang C 2017 Targeted soft biodegradable glycine/PEG/RGD-modified poly (methacrylic acid) nanobubbles as intelligent theranostic vehicles for drug delivery ACS Appl. Mater. Interfaces 9 35604–12

[56] Shen X, Li T, Chen Z, Geng Y, Xie X, Li S, Yang H, Wu C and Liu Y 2017 Luminescent/magnetic PLGA-based hybrid nanocomposites: a smart nanocarrier system for targeted codelivery and dual-modality imaging in cancer theranostics Int. J. Nanomed. 12 4299–322

[57] Bosca F, Bielecki P A, Exner A A and Barge A 2018 Porphyrin-loaded pluronic nanobubbles: a new US-activated agent for future theranostic applications Bioconjug. Chem. 29 234–40

[58] Ji G, Yang J and Chen J 2014 Preparation of novel curcuminloaded multifunctional nanodroplets for combining ultrasonic development and targeted chemotherapy Int. J. Pharm. 466 314–20

[59] Upadhyay A, Yagnik B, Desai P and Dalvi S V 2018 Microbubble-mediated enhanced delivery of curcumin to cervical cancer cells ACS Omega 3 12824–31

[60] Herman J G, Stadelman H L and Roselli C E 2009 Curcumin blocks CCL2-induced adhesion, motility and invasion, in part, through down-regulation of CCL2 expression and proteolytic activity Int. J. Oncol. 34 1319–27

[61] Hu H-J, Lin X-L, Liu M-H, Fan X-J and Zou W-W 2016 Curcumin mediates reversion of HGF-induced epithelialmesenchymal transition via inhibition of c-Met expression in DU145 cells Oncol. Lett. 11 1499–505

TABLES AND FIGURES

Table 1 Physico-chemical characteristics of nanobubble formulations. Results are shown as means ± SD (n=3) of three different preparations. Abbreviations: standard deviation (SD); and polydispesity index (PDI).

Nanobubble formulations	Average diameter ± SD (nm)	PDI	Z-potential ± SD (mV)	pH
Blank NBs	328.01 ± 5.10	0.19	−44.71 ± 4.22	6.90
Curc-NBs	348.45 ± 7.30	0.20	−53.27 ± 5.96	7.40

Table 2 Cell viability inhibition after the exposition of Curc or Curc-NBs to tumor cells.

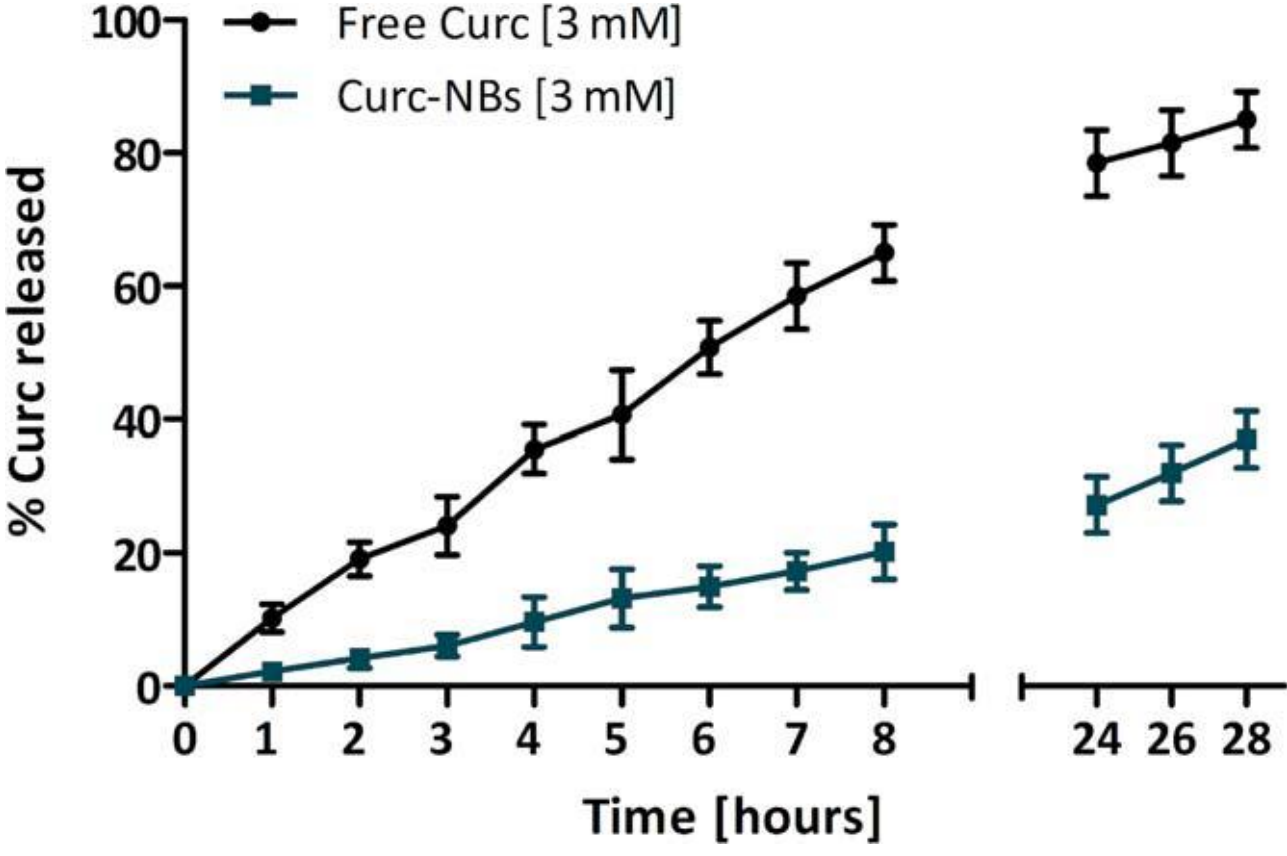|	% inhibition of viability					
	DU-145			**PC-3**		
	24h	48 h	72 h	24 h	48 h	72 h
Curc						
15 µM	39 ± 2	72 ± 1	75 ± 5	26 ± 2	60 ± 4	73 ± 2
10 µM	17± 4	33 ± 5	44 ± 5	11 ± 2	42 ± 3	58 ± 3
5 µM	9 ± 2	13 ± 4	10 ± 3	7 ± 1	20 ± 2	33 ± 3
1 µM	5 ± 2	4 ± 3	3 ± 1	3 ± 1	13 ± 4	15 ± 1
Curc-NBs						
15 µM	44 ± 5	80 ± 1*	87 ± 3*	37 ± 5*	74 ± 3*	88 ± 2
10 µM	31 ± 4*	55 ± 6**	61 ± 4**	27 ± 5*	59 ± 3**	71 ± 2**
5 µM	18 ± 6	19 ± 4	14 ± 6	6 ± 3	26 ± 4	42 ± 3
1 µM	14 ± 6	14 ± 6	6 ± 5	5 ± 2	18 ± 6	15 ± 5
Blank NBs	8 ± 5	9 ± 2	10 ± 4	3 ± 1	7 ± 5	8 ± 2

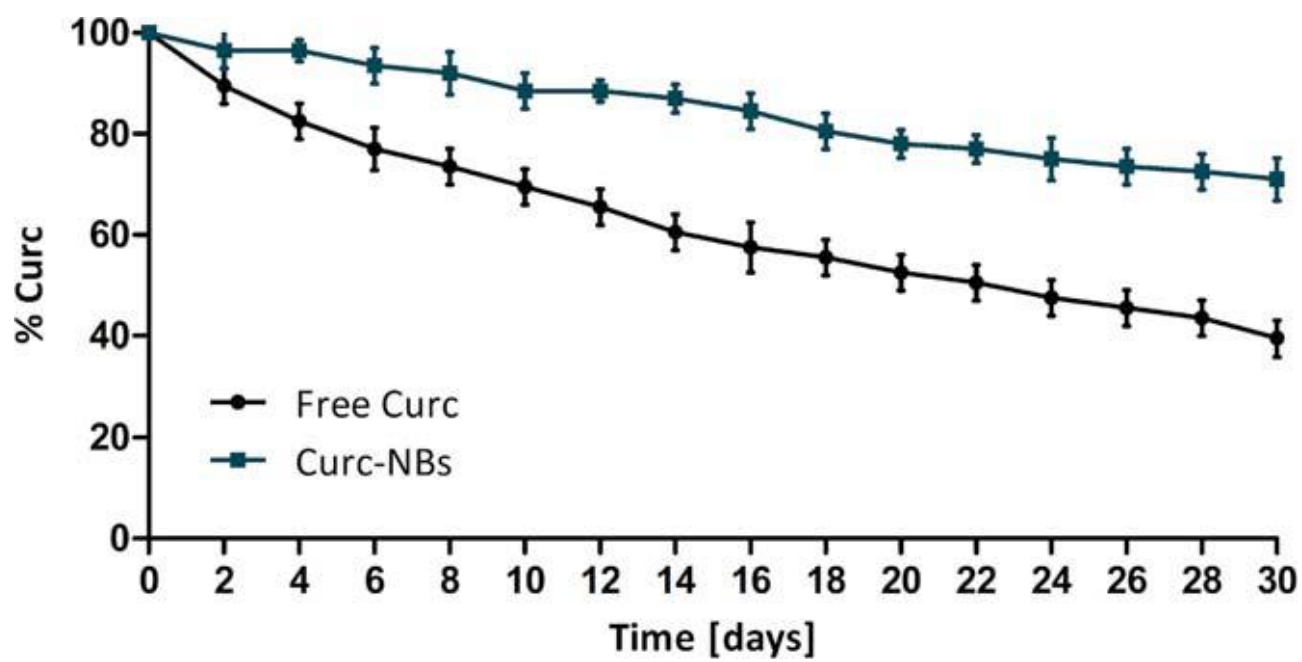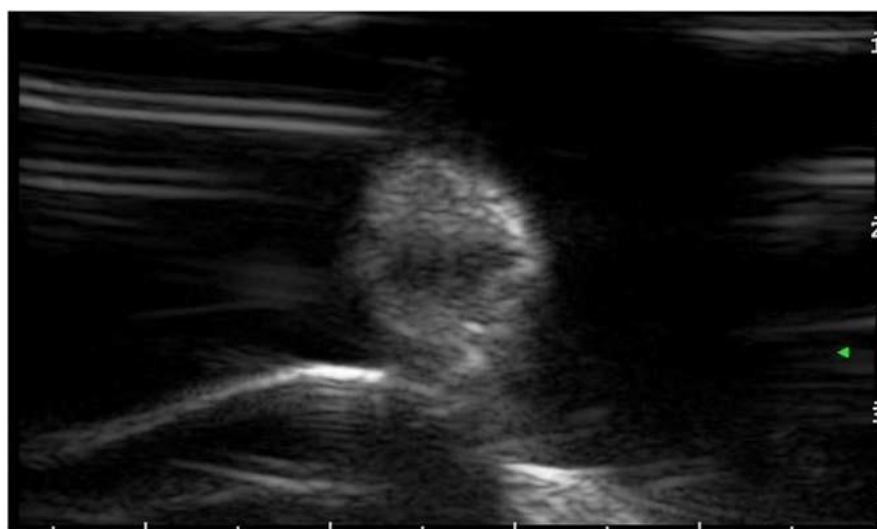Legend: *$p<0.05$ versus Curc; **$p<0.01$ versus Curc.

Figure 1

Figure 2

Figure 3

Figure 4
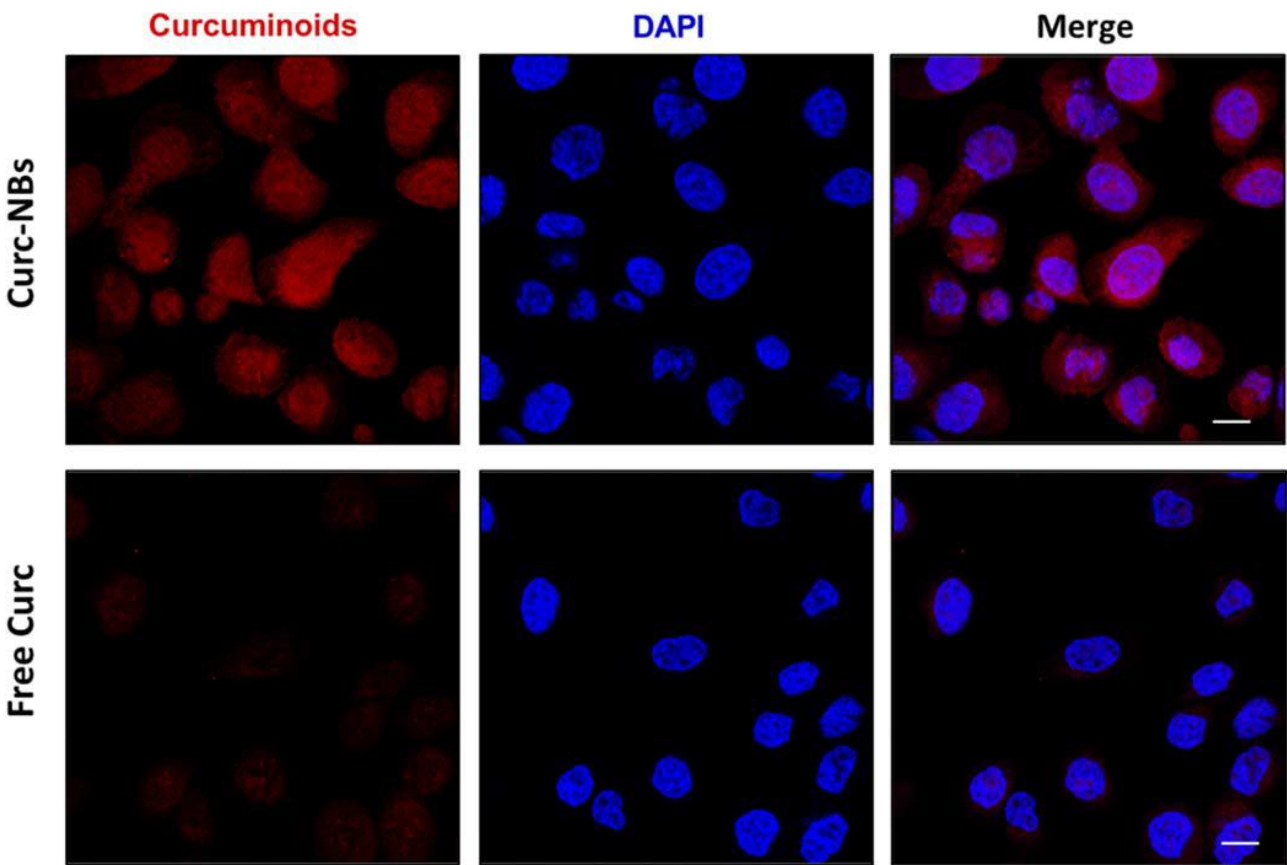
Figure 5
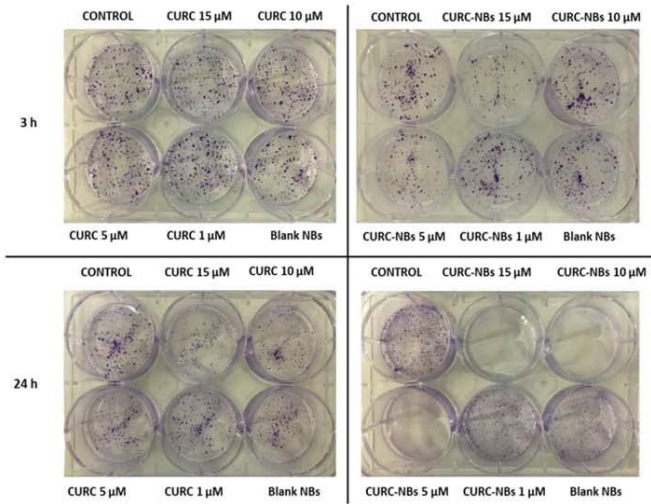
A

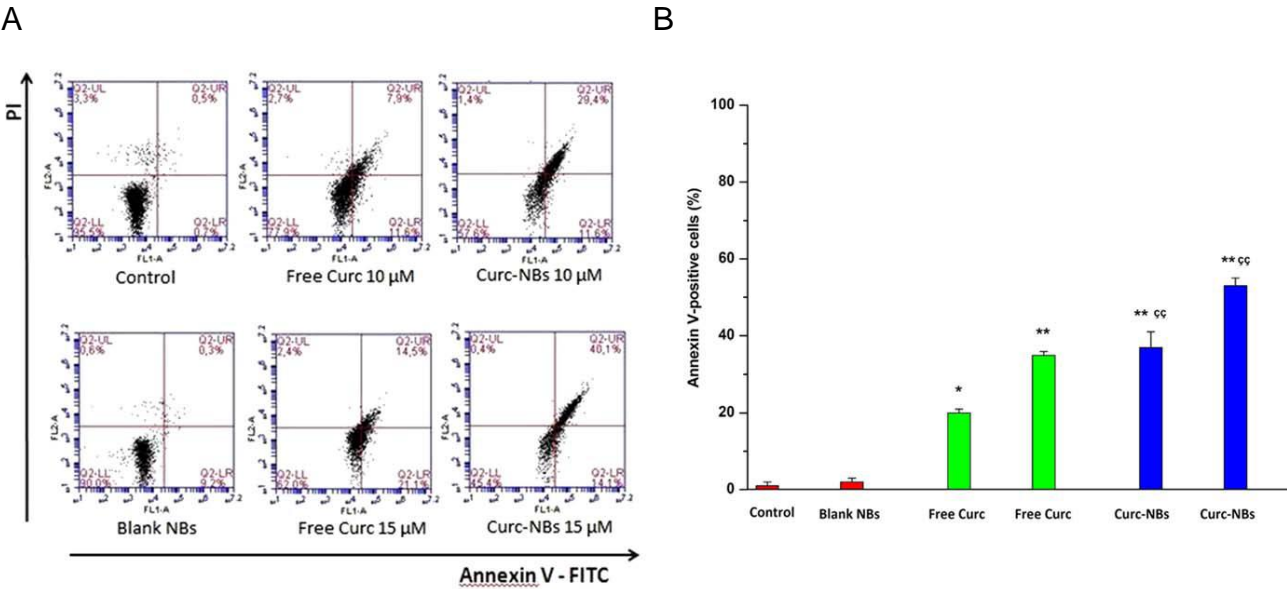
B

Figure 6
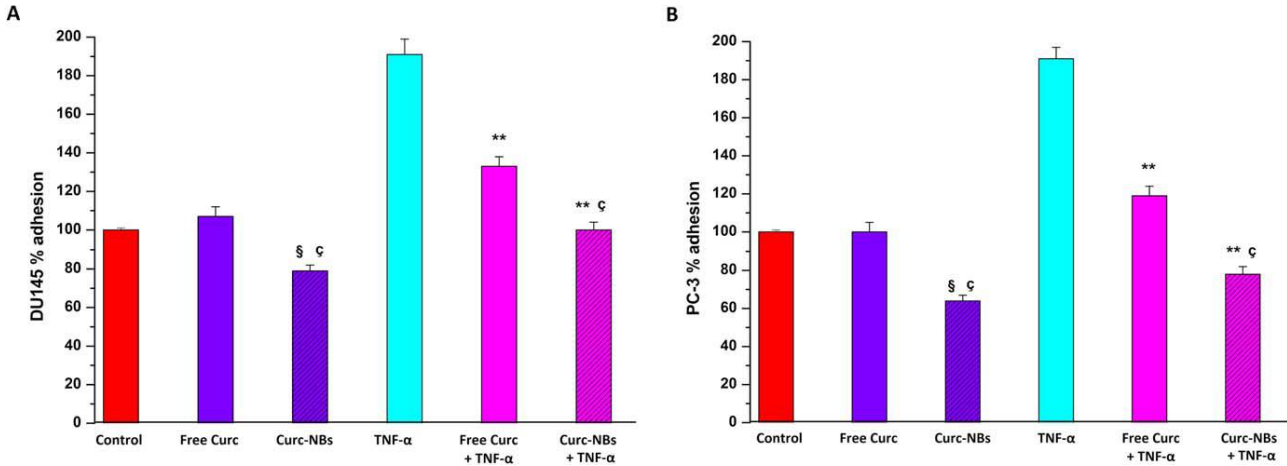
A

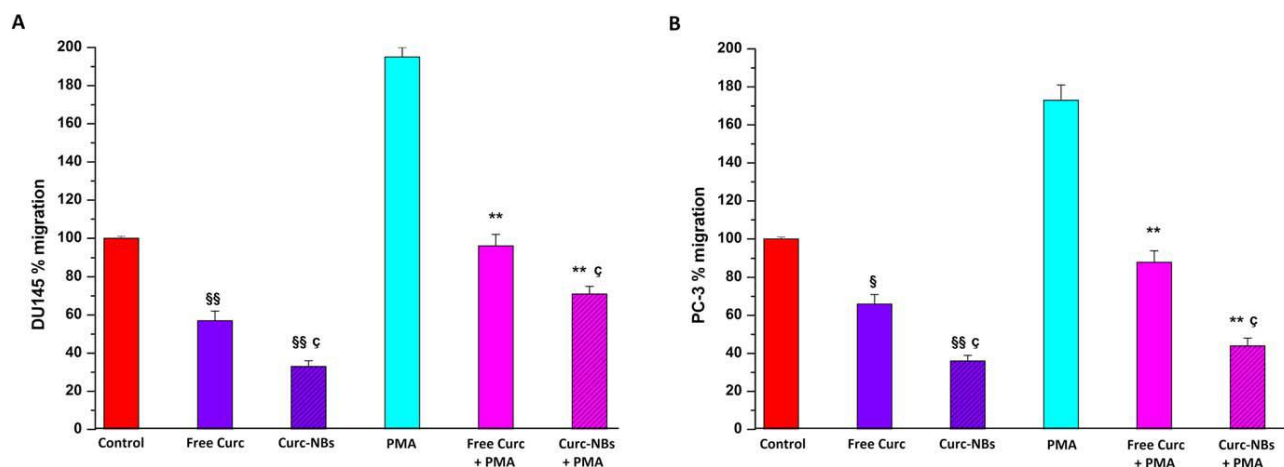
B

Figure 7

A

B
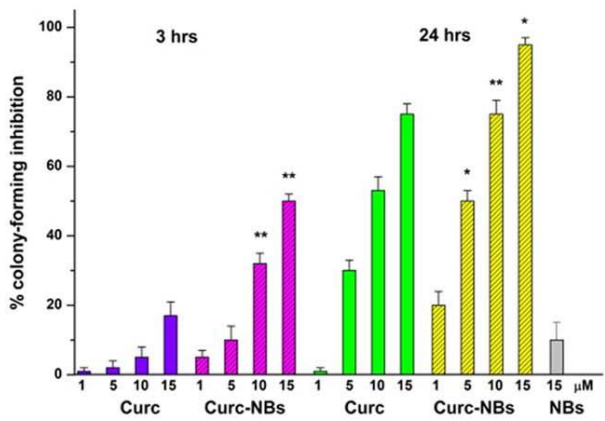
Figure 8

Figure legends

Figure 1. Curc-NBs released Curc in a sustained and prolonged over time manner. In vitro Curc release from Curc-NBs and Curc solution was evaluated up to 28 h. The results are presented as mean ± SD of three different experiments (n = 3).

Figure 2. Curc encapsulated in NBs presented a higher chemical stability over time. Chemical stability (expressed as percent of Curc remained) up to 30 days of Curc in solution and loaded in NBs was investigated. The results are shown as mean ± SD of three different experiments (n = 3).

Figure 3. Echogenic images of NBs, visualized using MyLab 25Gold (Esaote, Genova, Italy) sonograph.

Figure 4. Curc-NBs are avidly internalized by PC-3 cells. Curcuminoid-loaded NBs and curcuminoid solution were internalized into PC-3 cells after 1 h of incubation. Images are representative of three field per conditions (n = 3).

Figure 5. Inhibition of colony-forming assay by free Curc and Curc-NBs. PC-3 cells were treated with 1–15 µM of Curc solution and Curc- NBs, or untreated (control) for 3 or 24 h. Then, the cells were washed and allowed to growth for 7 d. Moreover, the cells were treated with blank NBs, at the dilution corresponding to that of Curc-NBs 15 µM. Panel A: percent of inhibition of colony-forming. The controls (untreated cells) were normalized to 100%, and the readings from treated cells were expressed as % of viability inhibition and are the mean ± SD. *p< 0.05 Curc-NBs versus Curc solution at the corresponding dilution; **p<0.01 Curc-NBs versus Curc at the corresponding dilution. Panel B: representative experiments of colony-forming were photographed.

Figure 6. Determination of apoptosis using a flow cytometry based Annexin V/IP assay. PC-3 cells were treated with 10 and 15 µM of Curc and Curc-NBs, or untreated (control) for 24 h. Moreover, the cells were treated with blank NBs, at the dilution corresponding to that of Curc- NBs 15 µM. Panel A: flow cytometry profiles of representative experiment. Panel B: summary of the Annexin V-FITC Apoptosis assay results of three independent experiments. Data are expressed as percentage and are the mean ± SD. *p < 0.05 **p . 0.01 versus control, çç . 0.01 versus Curc solution at the corresponding dilution.

Figure 7. Tumor cell adhesion to HUVEC induced by Curc and Curc-NBs. Panel A DU-145cells and Panel B PC-3 were treated with 5 µM of Curc solution and Curc-NBs, or untreated (control) for 30 min and then stimulated with TNF-α 10 ng ml−1. After 18 h, tumor cells were seeded and left to adhere for 1 h. Data are expressed as percentage of tumor cell adhesion on HUVEC and are the mean ± SD. § p <0.05 Curc-NBs versus control; **p <0.01 Curc-NBs and free Curc versus TNF-α; ç p <0.05 Curc-NBs versus free Curc at the corresponding dilution.

Figure 8. Tumor cell migration induced by Curc and Curc-NBs. Panel A DU145cells and Panel B PC-3 were treated with 5 µM of Curc solution and Curc-NBs, or untreated (control) and seeded in the upper chamber of a Boyden chamber in a serum-free medium. The cells were allowed to migrate for 18 h to the lower chamber containing PMA 10 ng ml−1 or FCS 20%. Data are expressed as percentage of tumor cell migration and are the mean ± SD. § p <0.05 Curc-NBs versus control; §§ p <0.05 Curc-NBs versus control; **p <0.01 Curc-NBs and free Curc versus PMA; ç p< 0.05 Curc-NBs versus free Curc at the corresponding dilution.